International Journal of GEOMATE, April, 2026 Vol.30, Issue 140, pp.104-114
ISSN: 2186-2982 (P), 2186-2990 (O), Japan, DOI: https://doi.org/10.21660/2026.140.g15283
Geotechnique, Construction Materials and Environment

MONTE CARLO–BASED ESTIMATION OF REGIONAL ECOSYSTEM PARAMETERS IN THE SETO INLAND SEA

* Yutaro Koga[1, 3], Yuichi Sato[2], Tomohito Matsuo[3] and Hikari Shimadera[3]

[1] Hyogo Prefectural Institute of Environmental Sciences, Japan; [2] Lake Biwa Environmental Research Institute, Japan; [3] Graduate School of Engineering, the University of Osaka, Japan

*Corresponding Author, Received: 30 May 2025, Revised: 07 Jan. 2026, Accepted: 10 Jan. 2026

ABSTRACT: This study developed and applied a Monte Carlo–based food-chain box model to identify region-specific ecosystem parameter sets for 13 sub-regions of the Seto Inland Sea. For each region, large ensembles of Monte Carlo simulations (approximately 10,000–700,000 realizations) were explored to identify 1,000 feasible parameter sets for 28 ecosystem parameters that simultaneously reproduced the observed ranges of dissolved inorganic nitrogen (DIN) concentrations and phytoplankton biomass in both the 1990s and the 2010s. This approach allowed parameter uncertainty to be systematically constrained using long-term monitoring data rather than subjective tuning. The estimated parameters exhibited clear inter-regional differences, particularly in the maximum growth rates of phytoplankton and zooplankton and in phytoplankton sinking velocities. These differences were consistent with observed regional variations in phytoplankton community composition, nutrient conditions, and physical environments. Overall, the results highlight the importance of region-specific ecosystem parameter settings for accurately simulating coastal ecosystem dynamics and for improving the reliability of high-resolution numerical models.

Keywords: Food Chain Model, Ecosystem Parameter, Monte Carlo Method, Seto Inland Sea

1. INTRODUCTION

Fisheries in coastal seas have developed through nutrient inputs from rivers and discharges, but fishery yields have declined worldwide due to ecosystem changes associated with climate change, overfishing, and water pollution [1]. Coastal seas are particularly sensitive to both natural variability and anthropogenic pressures because they receive substantial land-derived nutrient inputs while simultaneously being exposed to large climatic and physical fluctuations. As a result, management of coastal fisheries requires an integrated understanding of biogeochemical processes, ecosystem structure, and their responses to external forcings. Numerical ecosystem models are therefore widely used for coastal management. Previous studies have emphasized the importance of accurate parameter estimation in higher-trophic-level models and highlighted uncertainties caused by parameter and boundary-condition settings [2–6]. Similar challenges have also been reported in studies focusing on lower-trophic and microbial ecosystems, where environmental forcings such as light conditions strongly influence ecosystem functions and complicate parameter evaluation [7]. In particular, uncertainties in biological parameters often propagate nonlinearly through food-web interactions, leading to large uncertainties in simulated biomass and production at higher trophic levels. This issue has been recognized as a major limitation in applying ecosystem models to practical coastal management. Because ecosystem parameters vary both temporally and spatially, complex models with many parameters are not always practical, and simplified approaches are often more suitable for policy applications [8, 9].

Our previous study developed a Monte Carlo–based two-box food-chain model for Harima Nada in the eastern Seto Inland Sea, assigning parameter ranges to each box based on dominant phytoplankton groups and successfully reproducing water-quality changes in the 1990s and 2010s [10]. However, this approach still involved arbitrariness because the parameter ranges were manually specified, similar to conventional tuning practices. Such arbitrariness in defining parameter ranges makes it difficult to objectively evaluate parameter uncertainty and limits the transferability of the estimated parameters to other regions or environmental conditions. Reducing this subjectivity is therefore essential for establishing a more transparent and reproducible parameter estimation framework.

In addition, most ensemble calibration and data assimilation studies estimate a single parameter set for the entire model domain and therefore do not explicitly account for regional differences in ecosystem characteristics. In highly heterogeneous semi-enclosed systems such as the Seto Inland Sea—where environmental conditions differ markedly among bays and nadas—region-specific parameter estimation remains insufficiently explored.

In this study, we estimate region-specific ecosystem parameters across multiple sub-regions of the Seto Inland Sea using unified prior parameter ranges within a consistent Monte Carlo–based framework. We evaluate the model's ability to reproduce observed water-quality characteristics in

both the 1990s and the 2010s and analyze how differences in the estimated parameters relate to environmental conditions such as nutrient concentrations and phytoplankton community composition. The findings are expected to provide practical guidance for parameterizing high-resolution coastal models and offer engineering insights to support science-based coastal management.

2. RESEARCH SIGNIFICANCE

In this study, we propose a Monte Carlo–based parameter estimation framework to reduce subjectivity and estimate region-specific ecosystem parameters under observational constraints. By applying parameter distributions rather than single representative values, the framework is expected to support uncertainty-aware parameterization in high-resolution coastal models. For example, it can assist nutrient load reduction assessments by quantifying both expected water-quality improvements and associated uncertainty, thereby supporting science-based coastal management and engineering applications.

3. MODEL AND METHODS

3.1 Model Structure

The model is a box-type food-chain model consisting of five major components—nutrients, phytoplankton, zooplankton, planktivorous fish, and piscivorous fish—where each box is assumed to be a completely mixed layer. The food-chain model, originally developed for Lake Biwa and modified for Harima Nada, was further improved in this study by replacing total nitrogen (TN) with dissolved inorganic nitrogen (DIN), which is directly available to organisms [10, 11]. Seasonal variations were not considered; instead, the model reproduced the annual average conditions, and the calculation time step was set to one day. The schematic structure of the model is shown in Fig. 1, while the full mathematical formulations are provided in Table A1.

3.2 Study Area and Input Data

The study area covers the entire Seto Inland Sea. Based on differences in water quality characteristics—such as nutrient concentrations and phytoplankton biomass—the area was divided into 13 boxes, each representing a distinct region (Fig. 2).

The input data used in the model are summarized in Table 1, and seawater exchange volumes are listed in Table 2. Data for DIN, phytoplankton biomass (as chlorophyll-a), and transparency were interpolated from observations by the Ministry of the Environment of Japan and weighted using 500-m mesh bathymetry data from the Japan Oceanographic Data Center. The land-derived TN load for each bay and sea area was estimated using the LQ equations reported in the previous study, which represent empirical relationships between TN load and river discharge [12]. For the 2010s, riverine water inflow from major rivers was obtained from the data provided by the Ministry of Land, Infrastructure, Transport and Tourism of Japan. For small and medium-sized rivers, the inflow was estimated by scaling the discharge of nearby major rivers according to the ratio of watershed areas. The TN load in the 1990s was estimated by applying the ratio of land-derived loads reported by the Ministry of the Environment of Japan, relative to the values in the 2010s. The DIN load was then calculated by applying a DIN/TN ratio of 0.8, based on previous studies [13, 14]. The carbon-to-chlorophyll-a ratio (C/Chl.a) was set to 56.4, based on observations from the Seto Inland Sea [15].

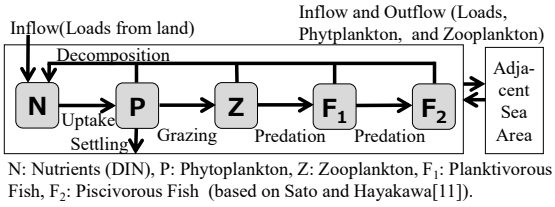

N: Nutrients (DIN), P: Phytoplankton, Z: Zooplankton, F_1: Planktivorous Fish, F_2: Piscivorous Fish (based on Sato and Hayakawa[11]).

Fig.1 Structure of the food chain model.

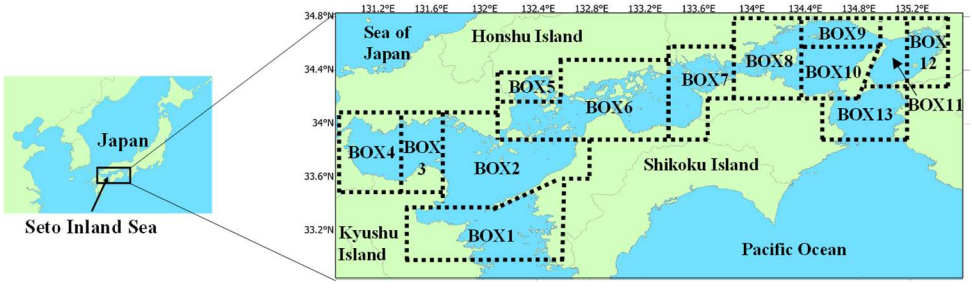

Fig.2 Study area consisting of 13 model boxes.

The compensation depth was then calculated as 2.7 times the transparency (SD), following a previous study [15]. SD for each box was estimated using Eq. (1), derived from the relationship between SD and chlorophyll-a concentration in each region [17, 18]. The empirical relationship used for estimating SD is expressed as:

$$\log(SD) = a - b \cdot \log(Chl.a) \quad (1)$$

where *SD* : Secchi disk transparency (m), *Chl.a* : Chlorophyll-a concentration (mg m^{-3}) and a, b : Empirically determined constants. Fig. 3 shows the relationship between SD and chlorophyll-a concentration for the 1990s and the 2010s in each box. In this study, a = 0.96, b = 0.40, and the coefficient of determination (R^2) = 0.77.

Table 1 Model input data

BOX	Vol.	Depth	DIN Cons.	Phyto-plankton	DIN from Land
	$\times10^{11}$ m^3	m	$\times10^{-2}$ gN m^{-3}	$\times10^{-2}$ gC m^{-3}	$\times10^{8}$ gN day^{-1}
1	1.82	60.5	5.6	5.5	0.18
			4.5	4.0	0.15
2	1.99	46.1	3.8	6.3	0.20
			3.8	6.0	0.13
3	0.27	23.9	1.7	7.9	0.07
			2.5	11	0.04
4	0.16	10.8	2.9	15	0.23
			2.4	13	0.12
5	0.05	17.2	8.5	23	0.24
			5.4	20	0.19
6	0.92	26.8	4.9	9.8	0.19
			4.1	9.1	0.17
7	0.26	16.4	5.9	14	0.49
			3.4	16	0.29
8	0.25	19.4	9.1	16	0.47
			5.1	15	0.19
9	0.18	21.9	8.2	12	0.58
			4.9	12	0.23
10	0.45	29.2	8.1	7.7	0.02
			5.3	7.7	0.01
11	0.33	39.6	10	19	0.10
			5.7	9.4	0.04
12	0.08	14.1	16	49	1.90
			8.1	24	0.74
13	0.75	43.7	9.7	6.4	1.00
			5.8	2.8	0.42
WB*	-	-	4.6	4.7	-
			4.3	3.4	
EB*	-	-	7.7	5.7	-
			5.5	3.6	

*WB: Western Boundary, EB: Eastern boundary

Note:
Upper row shows values for the 1990s, and lower row shows values for the 2010s.

To evaluate differences between the 1990s and the 2010s, the land-derived DIN load, the DIN inflow from adjacent waters, and the phytoplankton biomass in adjacent sea areas were varied between the two decades. In contrast, other input data, including water depth, water volume, and water-exchange rates, were commonly used for both periods. Exchange volumes were obtained from JCOPE2M [19, 20].

Table 2. Water exchange volumes between boxes.

from → to	Volume m^3/day
BOX1 → Western Boundary	8.56×10^{9}
Western Boundary → BOX1	9.40×10^{9}
BOX 1 → BOX 2	6.43×10^{9}
BOX 2 → BOX 1	5.58×10^{9}
BOX 2 → BOX 3	8.17×10^{8}
BOX 3 → BOX 2	8.17×10^{8}
BOX 4 → BOX 3	5.57×10^{8}
BOX 3 → BOX 4	5.57×10^{8}
BOX 2 → BOX 6	1.38×10^{9}
BOX 6 → BOX 2	5.35×10^{8}
BOX 5 → BOX 6	4.36×10^{8}
BOX 6 → BOX 5	4.36×10^{8}
BOX 6 → BOX 7	1.38×10^{9}
BOX 7 → BOX 6	5.36×10^{8}
BOX 7 → BOX 8	1.17×10^{9}
BOX 8 → BOX 7	3.21×10^{8}
BOX 8 → BOX 9	3.29×10^{8}
BOX 9 → BOX 8	1.84×10^{8}
BOX 8 → BOX 10	1.71×10^{9}
BOX 10 → BOX 8	1.01×10^{9}
BOX 9 → BOX 10	1.07×10^{9}
BOX 10 → BOX 9	1.04×10^{9}
BOX 9 → BOX 11	4.77×10^{8}
BOX 11 → BOX 9	3.68×10^{8}
BOX 10 → BOX 13	9.91×10^{8}
BOX 13 → BOX 10	2.55×10^{8}
BOX 11 → BOX 12	1.20×10^{9}
BOX 12 → BOX 11	1.20×10^{9}
BOX 11 → BOX 13	1.02×10^{9}
BOX 13 → BOX 11	9.10×10^{8}
BOX 13 → Eastern Boundary	1.56×10^{10}
Eastern Boundary → BOX 13	1.48×10^{10}

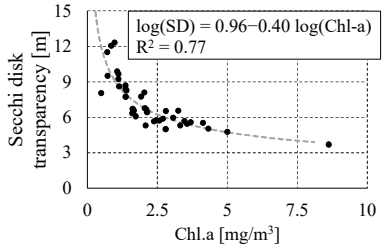

Fig.3 The relationship between SD and Chl.a concentration for the 1990s and the 2010s in each box

3.3 Calculation Procedure

To estimate ecosystem parameters for each water region, variation ranges for all 28 parameters were defined based on published laboratory measurements and previous ecosystem modeling studies (Table 3) [3, 11, 21–25]. For each parameter, the selected minimum and maximum values were chosen to cover the majority of values reported in the literature and avoid unrealistically narrow bounds that would restrict the Monte Carlo sampling. When published values differed substantially among studies, the range was slightly widened to account for environmental variability across the Seto Inland Sea. In some cases (e.g., maximum growth rate, respiration rate), the adopted ranges exceeded published values to ensure numerical stability during simulations.

The following procedure was then applied. Each simulation continued until the system reached a periodic steady state. Steps 1 and 2 were repeated until 1,000 valid parameter sets were obtained.

Step 1:

Parameter values were randomly sampled from these ranges, and two separate simulations were conducted using boundary conditions representing the 1990s and the 2010s, respectively.

Step 2:

Each simulation result was accepted only if it satisfied the following two criteria, evaluated under periodic steady-state conditions.

(i) The average values of DIN concentration and biomasses at steady state fall within the observed ranges for the 1990s and 2010s.

(ii) The coefficient of variation (standard deviation divided by the mean) for DIN concentration and each biomass at steady state in the 2010s simulation is 0.2 or less.

In this study, the parameter same set was used for both the 1990s and the 2010s. In our previous study, the ecosystem parameter ranges were adjusted for each box based on the dominant phytoplankton types to reproduce water quality in each box [10]. In contrast, this study employed uniform variation ranges across all boxes, as widely as possible based on literature values, to minimize subjectivity in the parameter estimation process.

For simplicity, water quality within each box was simulated independently without coupling with adjacent boxes. Model reproducibility was evaluated by comparing the simulated DIN concentrations and phytoplankton biomasses with observed values.

The ecological consistency of the estimated parameters was examined in relation to phytoplankton community composition, as well as associated physical and water-quality characteristics.

Table 3 Variation ranges for 28 ecosystem parameters.

Category	Name	Unit	Min.	Max.	Literature Value
Phyto-plankton	maximum growth rate	day^{-1}	0.3	3.5	1-5 [11], 2.5-3 [3], 0.5-2.4 [21]
	exocytosis rate	day^{-1}	0.01	0.3	0.01-0.1 [11]
	maximum nutrients uptake rate	$gN\ gC^{-1}\ day^{-1}$	0.1	1.5	0.01-0.1 [11]※
	half saturation constant	$gN\ m^{-3}$	0.01	1	0.0005-0.01 [11]※, 0.003-0.589 [22]
	congestion effect constant	$m^3\ gC^{-1}$	0.1	2	0.1-1 [11]
	respiration rate	day^{-1}	0.01	0.3	0.01-0.2 [11], 0.02-0.25 [3], 0.01-0.037 [21]
	mortality rate	day^{-1}	0.01	0.3	0.01-0.1 [11], 0.05-0.2 [23]
	deposition rate	$m\ day^{-1}$	0.01	5	0.05-0.4 [11], 0.5 [3], 3.2[24]
	maximum N:C ratio	-	0.17	0.2	0.02-0.03 [11]※, 0.18-0.21 [3]
	minimum N:C ratio	-	0.02	0.06	0.005-0.01 [11]※, 0.06-0.11 [3], 0.2 [21]
Zoo-plankton	maximum growth rate	day^{-1}	0.1	0.8	0.2-0.4 [11], 0.2-1.1 [21]
	assimilation rate	-	0.6	0.8	0.4-0.9 [11]
	half saturation constant	$gC\ m^{-3}$	0.09	0.18	0.05-0.2 [11]
	respiration rate	day^{-1}	0.01	0.03	0.005-0.05 [11], 0.04-0.23 [21]
	mortality rate	day^{-1}	0.02	0.07	0.005-0.05 [11]
	N:C ratio	-	0.06	0.12	0.015-0.035 [11]※, 0.12 [21]
Plankti-vorous Fish	maximum growth rate	day^{-1}	0.11	0.16	0.1-0.3 [11]
	assimilation rate	-	0.7	0.9	0.4-0.9 [11]
	half saturation constant	$gC\ m^{-3}$	0.02	0.05	0.05-0.15 [11]
	respiration rate	day^{-1}	0.004	0.02	0.002-0.015 [11]
	mortality rate	day^{-1}	0.012	0.025	0.002-0.01 [11]
	N:C ratio	-	0.07	0.13	0.04-0.06 [11]※, 0.2[25]
Pisci-vorous Fish	maximum growth rate	day^{-1}	0.06	0.12	0.1-0.3 [11]
	assimilation rate	-	0.8	0.95	0.4-0.9 [11]
	half saturation constant	$gC\ m^{-3}$	0.07	0.11	0.02-0.1 [11]
	respiration rate	day^{-1}	0.001	0.004	0.002-0.015 [11]
	mortality rate	day^{-1}	0.003	0.008	0.001-0.005 [11]
	N:C ratio	-	0.04	0.1	0.04-0.06 [11]※, 0.2[25]

※values for phosphorus

4. RESULTS AND DISCUSSION

4.1 Model Reproducibility and Regional Water Quality Characteristics

Comparisons between simulated and observed values of DIN concentrations and phytoplankton biomass for the 1990s and the 2010s are shown in Fig. 4. For each box, approximately 10,000 to 700,000 Monte Carlo simulations were performed to obtain 1,000 valid parameter sets. The figure presents boxplots of 1,000 simulation results and 10 years of observational data, along with their respective averages. Because only simulations within the observational ranges were accepted as valid, the results reflect the characteristic water quality conditions of each box. In particular, BOX12 exhibited a much wider observational range than other boxes, resulting in a relatively larger difference between simulated and observed mean values.

In the 1990s, compared to the 2010s, DIN concentrations showed small changes in the western boxes (BOX1–5), while higher values were observed in the eastern side of the Seto Inland Sea (BOX6–13). Phytoplankton biomass, on the other hand, increased significantly in BOX12 and 13 compared to the 2010s.

Phytoplankton biomass generally ranged from 0.1 to 0.2 mgC L^{-1}, but was below 0.05 mgC L^{-1} in BOX1 and 13, and reached 0.24 mgC L^{-1} in BOX12. The high DIN concentration and phytoplankton biomass in Box 12 were mainly attributed to the large nutrient inputs from the Yodo River, a major river flowing through the Osaka urban area.

Because only parameter sets that reproduced the observed ranges for both the 1990s and the 2010s were accepted through the Monte Carlo selection process, the final simulations closely matched the observed water-quality characteristics across all boxes. We therefore obtained parameter sets that consistently reproduced the observed ranges for both decades, successfully capturing the distinct regional water-quality patterns of the Seto Inland Sea.

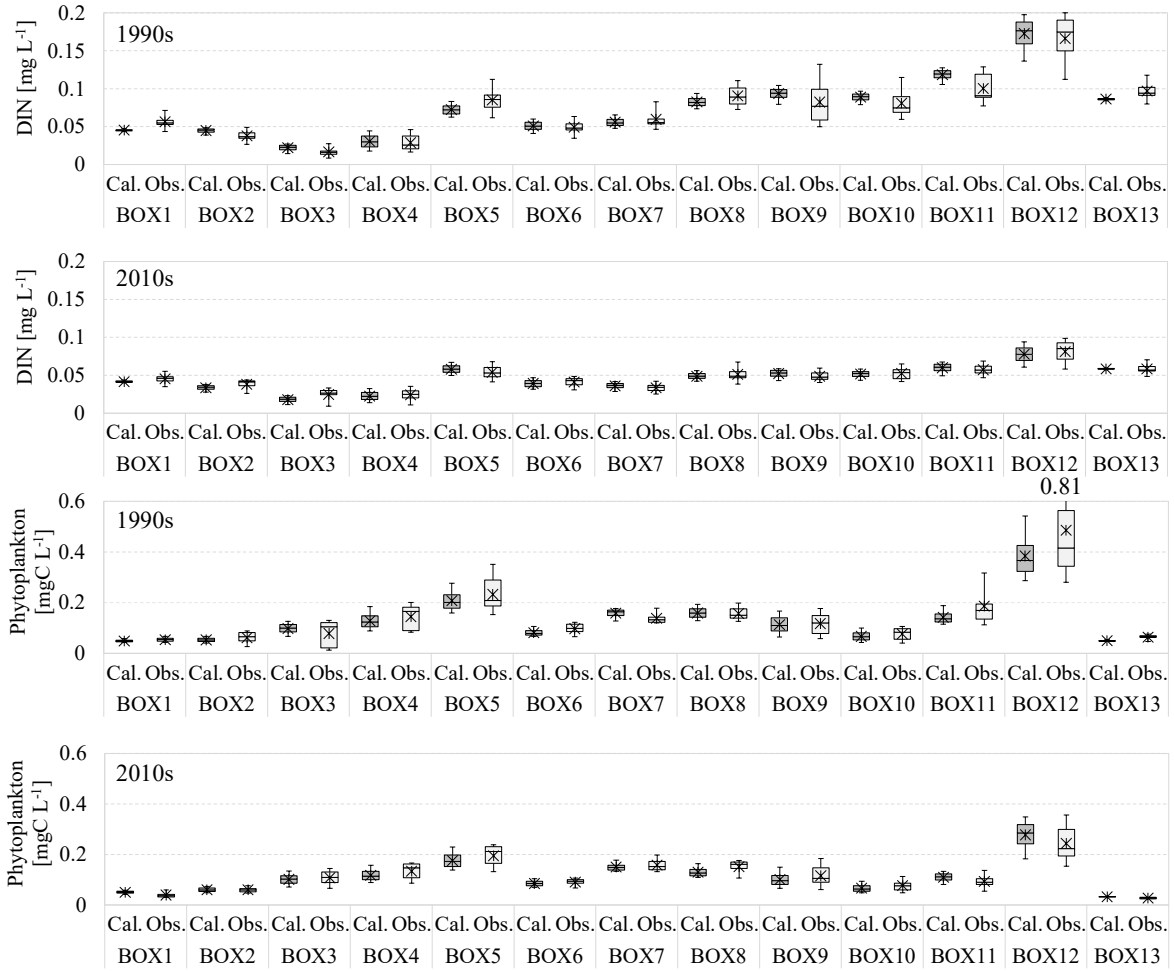

The top and bottom of the box represent 75th and 25th percentiles respectively. The top and bottom of the vertical line represent 95th and 5th percentiles. The inner line is the median and the asterisk represents the average.

Fig.4 Comparison of calculated and observed DIN concentrations between the 1990s and the 2010s.

4.2 Evaluation of Ecosystem Parameters

Fig. 5 presents the phytoplankton species composition in the 2010s provided by the Ministry of the Environment of Japan, spatially interpolated and adjusted for each box, and Fig. 6 shows key ecosystem parameters that exhibited notable differences among the boxes. Fig. 7 illustrates the relationships between the mean values of the ecosystem parameters shown in Fig. 6 and independent environmental indicators.

The maximum phytoplankton growth rate was high in BOX1–6 and BOX11–13. BOX3, BOX4, BOX6, and BOX11–13 were dominated by diatoms (Fig. 7(a)), which generally have high intrinsic growth rates, explaining the elevated maximum phytoplankton growth rate. In BOX5, the dominance of diatoms was somewhat lower than in other boxes; however, the high DIN concentrations likely supported a high phytoplankton growth rate [26]. In BOX1 and BOX2, the model estimated relatively high maximum phytoplankton growth rate despite the low proportion of diatoms. Both boxes were characterized by high water transparency and low phytoplankton biomass, providing a favorable light environment that can support high growth rates even without strong diatom dominance [27]. In contrast, BOX7 exhibited a lower maximum phytoplankton growth rate and a low minimum NC ratio, indicating high nitrogen-use efficiency. This parameter pattern corresponds to the observed condition in which relatively high phytoplankton biomass is maintained despite low DIN concentrations. In addition, because the Seto Inland Sea is generally influenced by an eastward residual current, a large amount of diatoms produced in BOX6 may have been transported into BOX7 and subsequently replaced by other taxa while being advected toward BOX8. In BOX9 and BOX10, the estimated parameters did not conform to the interpretations described above. In such cases, the estimated growth rate parameters may partially compensate for uncertainties inherent in the input data or model structure, such as water exchange rates, nutrient loading, or light conditions. Therefore, although the regional differences in the estimated parameters are broadly consistent with known ecological characteristics of the dominant phytoplankton groups, caution is required when interpreting these parameters as direct indicators of the intrinsic physiological traits of phytoplankton.

Based on Fig. 7(b), a tendency was observed whereby regions with higher DIN concentrations exhibited lower estimated nutrient uptake rates. This tendency is consistent with physiological plasticity and adaptive strategies, in which nutrient acquisition capacity (e.g., maximum uptake rate or affinity) is enhanced under nutrient-poor conditions, whereas high uptake capacity is not required in nutrient-rich environments [28]. In addition, BOX13, located in the Kii Channel, is strongly influenced by exchange with offshore waters and showed a high proportion of offshore-type Chaetoceros. This genus is adapted to oligotrophic offshore environments and is known to have lower nutrient uptake capacity than coastal diatoms, which explains the relatively low nutrient uptake rate estimated by the model for this region [29].

Regions with a high proportion of diatoms tended to exhibit faster sinking rates (Fig. 7(c)), consistent with the well-established understanding that diatom-dominated communities experience enhanced gravitational settling due to their heavier cell structures. In contrast, BOX6 exhibited a relatively low sinking rate despite the strong dominance of diatoms. This region contains numerous small islands and is influenced by comparatively strong tidal currents. Such intensified water-column mixing likely reduced effective sedimentation, resulting in the lower sinking rates estimated by the model [30].

The maximum zooplankton growth rate tended to increase as DIN concentration decreased (Fig. 7(d)). Although zooplankton feed on phytoplankton and therefore are not directly related to ambient DIN concentration, regions with higher DIN levels may favor larger phytoplankton size structures. Such size enlargement could reduce prey palatability and feeding efficiency for zooplankton, resulting in lower estimated maximum growth rates [30]. In BOX13, relatively low maximum zooplankton growth rates were estimated despite low DIN concentrations. As discussed above, this region is characterized by a high proportion of offshore-type Chaetoceros, which likely includes relatively large cells and chain-forming species. These characteristics may have reduced food availability and prey accessibility for zooplankton, leading to the lower growth rates estimated by the model.

These region-specific parameter characteristics are important for engineering-oriented coastal modeling. The common assumption of spatially uniform biological parameters in high-resolution three-dimensional models may lead to biased representations of phytoplankton dynamics, nutrient cycling, and sedimentation processes in heterogeneous systems such as the Seto Inland Sea. Applying the region-specific ranges of ecosystem parameters estimated in this study as initial values or spatial constraints in ecosystem models coupled with three-dimensional hydrodynamic models is expected to improve model reproducibility.

These parameters should be interpreted as effective values that reflect uncertainties in the structure of the present model and its input conditions. In addition, the proposed parameter estimation framework is applicable to scenario analyses for nutrient management, wastewater discharge planning, and environmental impact

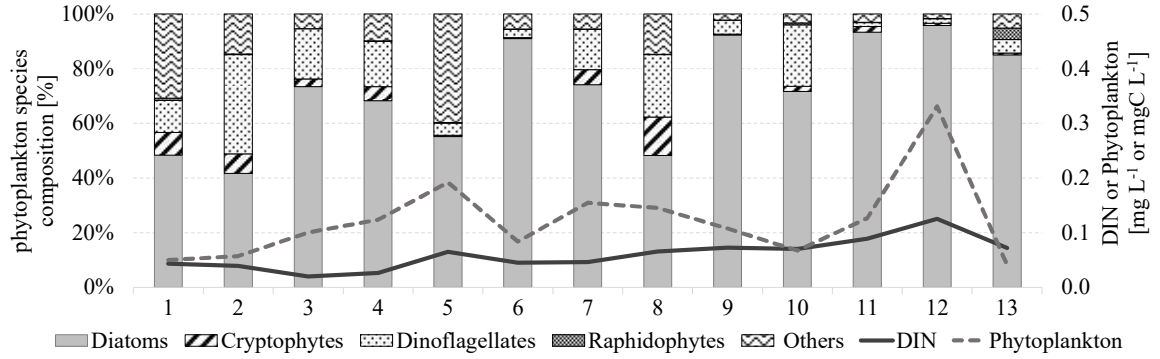

Fig. 5 Observed phytoplankton species composition, averaged across the 1990s and 2010s.

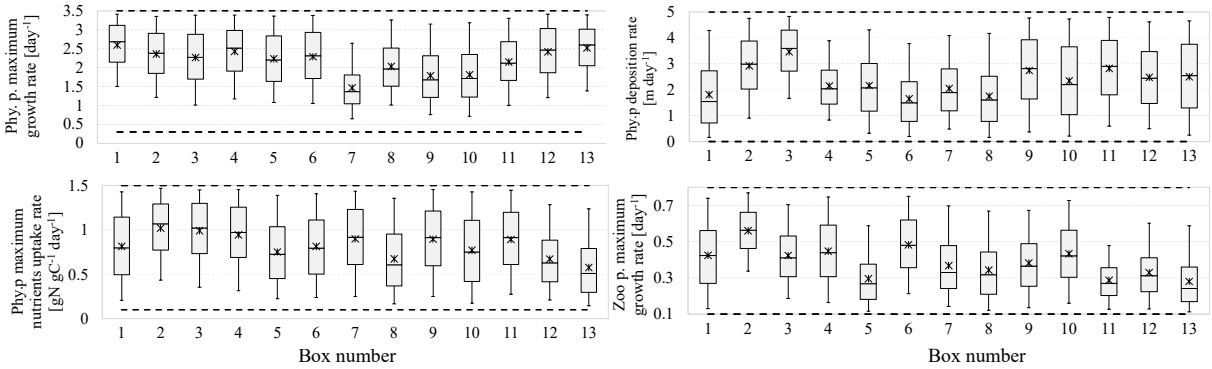

The top and bottom of the box represent 75th and 25th percentiles respectively. The top and bottom of the vertical line represent 95th and 5th percentiles. The inner line is the median and the asterisk represents the average. The dashed lines indicate the maximum and minimum values of the predefined parameter range.

Fig. 6 Estimated ecosystem parameters showing regional variations among 13 boxes.

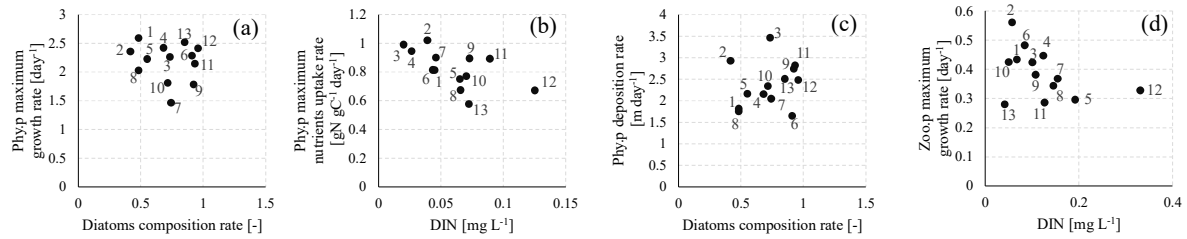

Fig.7 Relationships between estimated ecosystem parameters and environmental indicators.

assessment, supporting decision-making under uncertainty.

5. CONCLUSION

This study estimated ecosystem parameters for multiple regions of the Seto Inland Sea using a Monte Carlo–based food-chain model. The model successfully reproduced key water-quality characteristics observed in both the 1990s and 2010s, including DIN concentrations and phytoplankton biomass. The estimated parameters captured regional differences in phytoplankton community structure, nutrient conditions, biomass levels, and physical environments such as tidal currents, and were broadly consistent with known ecological traits such as growth and sinking characteristics.

These results demonstrate that region-specific ecosystem parameters are essential for realistically simulating coastal ecosystem dynamics in heterogeneous systems. Although the estimated parameters should be interpreted as effective values that incorporate uncertainties arising from model structure and input conditions, the proposed framework presents a practical and transparent approach that has the potential to contribute to improving the reliability of high-resolution numerical

models. This approach also offers a useful basis for scenario analyses related to nutrient management and environmental assessment in eutrophic coastal seas.

6. ACKNOWLEDGMENTS

This research was performed by the Environment Research and Technology Development Fund (JPMEERF24S12302) of the Environmental Restoration and Conservation Agency provided by the Ministry of the Environment of Japan.

7. REFERENCES

1. Jackson J.B.C., Kirby M.X., Berger W.H., Bjorndal K.A., Botsford L.W., Bourque B.J., Bradbury R.H., Cooke R., Erlandson J., Estes J.A., Hughes T.P., Kidwell S., Lange C.B., Lenihan H.S., Pandolfi J.M., Peterson C.H., Steneck R.S., Tegner M.J., and Warner R.R., Historical Overfishing and the Recent Collapse of Coastal Ecosystems. Science, 293(5530) 2001, pp. 629-638. https://doi.org/10.1126/science.1059199
2. Kishi M.J., Ito S., Megrey B.A., Rose K.A., and Werner F.E., A Review of the NEMURO and NEMURO.FISH Models and Their Application to Marine Ecosystem Investigations. Journal of Oceanography, 67(1) 2011, pp. 3-16. https://doi.org/10.1007/s10872-011-0009-4
3. Suzuki M., Nakatani Y., and Koga Y., Evaluating the Effects of Operations to Increase Nitrogen Discharge from Sewage Treatment Plants on Concentrations of Organic Matter and Nutrients in Surface Water at Harima-nada in the Seto Inland Sea. Journal of Japan Society on Water Environment, 43(2) 2020, pp. 43-53. https://doi.org/10.2965/jswe.43.43
4. Singh T., Counillon F., Tjiputra J., Wang Y., and Gharamti M.E., Estimation of Ocean Biogeochemical Parameters in an Earth System Model Using the Dual One-Step-Ahead Smoother: A Twin Experiment. Frontiers in Marine Science, 9 2022, pp. 775394. https://doi.org/10.3389/fmars.2022.775394
5. Bopp L., Resplandy L., Orr J.C., Doney S.C., Dunne J.P., Gehlen M., Halloran P., Heinze C., Ilyina T., Séférian R., and Tjiputra J., Multiple Stressors of Ocean Ecosystems in the 21st Century: Projections with CMIP5 Models. Biogeosciences, 10(10) 2013, pp. 6225–6245. https://doi.org/10.5194/bg-10-6225-2013
6. Losa S.N., Kivman G.A., and Ryabchenko V.A., Weak Constraint Parameter Estimation for a Simple Ocean Ecosystem Model: What Can We Learn About the Model and Data? Journal of Marine Systems, 45(1-2) 2004, pp. 1-20. https://doi.org/10.1016/j.jmarsys.2003.08.005
7. Nishimura F., Influence of Light on a Microbial River Water Ecosystem and Its Self-Purification Capacity. International Journal of GEOMATE, 20(81) 2021, pp. 146–152. https://doi.org/10.21660/2021.81.GX315
8. Uchida T., Ukita M., Sekine M., and Nakanishi H., The Study on the Nonlinear Characteristics of Water Quality in Eutrophic Sea Areas and Their Modeling. Journal of Japan Society of Civil Engineers, 503(2) 1994, pp. 187-195. (in Japanese)
9. Gerhard M., Koussoroplis A.M., Raatz M., Pansch C., Fey S.B., Vajedsamiei J., Calderó-Pascual M., Cunillera-Montcusí D., Juvigny-Khenafou N. P. D., Polazzo F., Thomas P. K., Symons C. C., Beklioğlu M., Berger S. A., Chefaoui R. M., Ger K. A., Langenheder S., Nejstgaard J. C., Ptacnik R., and Striebel M., Environmental variability in aquatic ecosystems: Avenues for future multifactorial experiments. Limnology and Oceanography Letters, 8(2) 2023, pp. 247-266. https://doi.org/10.1002/lol2.10286
10. Koga Y., Shimadera H., Sato Y., Pintos Andreoli V., Suzuki M., Matsuo T., and Kondo A., Evaluating the effects of land-derived nutrient load on nutrient and ecosystem production at Harima Nada in Seto Inland Sea using food chain model, Journal of Japan Society on Water Environment, 47(5) 2024, pp. 151-161. https://doi.org/10.2965/jswe.47.151
11. Sato Y., and Hayakawa K., Effect of nutrient loads on upper trophic level species in Lake Biwa: Analysis using food chain model by Monte Carlo method, Journal of Japan Society on Water Environment, 42(4) 2019, pp. 133-143. https://doi.org/10.2965/jswe.42.133
12. Kashima C., Nakatani Y., Higashi H., and Akiyama C., Estimation of the L–Q equations for each sea area in the Seto Inland Sea, Journal of Japan Society of Civil Engineers, 81(16) 2025, pp. 1-7. https://doi.org/10.2208/jscejj.24-16119
13. Koga Y., Suzuki M., and Pintos V., Analysis of nitrogen and phosphorus load dynamics in Kako and Ibo River basins during flood events, Journal of Japan Society of Hydrology and Water Resources, 35(1) 2022, pp. 32-40. https://doi.org/10.3178/jjshwr.35.32
14. Nakatani Y., Kawasumi R., and Nishida S., Change of inflow load and water environment in Osaka Bay, Journal of Japan Society of Civil Engineers, 67(2) 2011, pp. I_886-I_890. https://doi.org/10.2208/kaigan.67.I_886
15. Tada K., and Morishita M., The changes of environmental chemical conditions and biomass on lower trophic levels in a coastal bay, Bulletin of the Faculty of Agriculture, Kagawa University, 49(1) 1997, pp. 35-47. (in Japanese)
16. Tsuda R., Measurements of underwater spectral

irradiance in Lake Biwa. Japanese Journal of Limnology, 41(2) 1980, pp. 57-67 https://doi.org/10.3739/rikusui.41.57
17. Lorenzen C.J., Surface chlorophyll as an index of the depth, chlorophyll content, and primary productivity of the euphotic layer. Limnology and Oceanography, 15(3) 1970, pp. 479-480. https://doi.org/10.4319/lo.1970.15.3.0479
18. Carlson R.E., A trophic state index for lakes. Limnology and Oceanography, 22(2) 1977, pp. 361-369. https://doi.org/10.4319/lo.1977.22.2.0361
19. Miyazawa Y., Kuwano-Yoshida A., Doi T., Nishikawa H., Narazaki T., Fukuoka T., and Sato K., Temperature profiling measurements by sea turtles improve ocean state estimation in the Kuroshio–Oyashio Confluence region, Ocean Dynamics, 69 2019, pp. 267-282. https://doi.org/10.1007/s10236-018-1238-5
20. Miyazawa Y., Sergey M.V., Miyama T., Xinyu G., Hihara T., Kiyomatsu K., Kachi M., Kurihara Y., and Murakami H., Assimilation of high-resolution sea surface temperature data into an operational nowcast/forecast system around Japan using a multi-scale three dimensional variational scheme, Ocean Dynamics 67 2017, pp. 713-728. https://doi.org/10.1007/S10236-017-1056-1
21. Lee I., Sekine M., Ukita M., and Nakanishi H., Analysis of Fisheries Stocks in the Seto Inland Sea by Using the Shallow Sea Ecological Model. Journal of the Japan Society of Civil Engineers, 566(3) 1997, pp. 81-93. https://doi.org/10.2208/jscej.1997.566_81
22. Imamura M., and Matsunashi S., Response of Coastal Water Quality to Reduction of Nutrients Loading: Analysis of Lower Trophic Ecosystem Model with Phytoplankton Species Composition. Journal of the Japan Society for Marine Surveys and Technology, 18(2) 2006, pp. 11-26. https://doi.org/10.11306/jsmst.18.2_11
23. Taylor A.H., Watson A.J., Ainsworth M., Robertson J.E., and Turner D.R., A modelling investigation of the role of phytoplankton in the balance of carbon at the surface of the North Atlantic. Global Biogeochemical Cycles, 5(2) 1991, pp. 151-171. https://doi.org/10.1029/91GB00305
24. Watanabe T., Okuyama Y., Aritomi Y., Tsuji M., Tuge R., Oyagi M., and Chiba S., The Study on Sedimentation Velocity of Organic Matter in Ise Bay. Annual Report of Mie Environmental Conservation Research Institute, 22 2020, pp. 38-47.(in Japanese)
25. Koga N., Niimi H., Ihara H., Yamaguchi N., Yamane T., and Kusaba T., Acid Detergent-Soluble Organic Nitrogen Contents in Various Soil Organic Amendments: Trends of Amendment Types and Relationships with C/N Ratios. Japanese Journal of Soil Science and Plant Nutrition, 90(2) 2019, pp. 107-115. https://doi.org/10.20710/dojo.90.2_107
26. Chan A.T., Comparative Physiological Study of Marine Diatoms and Dinoflagellates in Relation to Irradiance and Cell Size. II. Relationship Between Photosynthesis, Growth, and Carbon/Chlorophyll a Ratio. Journal of Phycology, 16(3) 1980, pp. 428-432. https://doi.org/10.1111/j.1529-8817.1980.tb03056.x
27. Geider R. J., Light and temperature dependence of the carbon to chlorophyll a ratio in microalgae and cyanobacteria: implications for physiology and growth of phytoplankton. New Phytologist, 106 1987, pp. 1-34. https://doi.org/10.1111/j.1469-8137.1987.tb04788.x
28. Bonachela J.A., Raghib M., and Levin S.A., Dynamic model of flexible phytoplankton nutrient uptake. Proceedings of the National Academy of Sciences of the United States of America, 108(51) 2011, pp. 20633-20638. https://doi.org/10.1073/pnas.1118012108
29. Harrison P. J., Parslow J. S., and Conway H. L., Determination of nutrient uptake kinetic parameters: a comparison of methods. Marine Ecology Progress Series, 52 1989, pp. 301-312. https://doi.org/10.3354/meps052301
30. Kiørboe T., and Saiz E., Planktivorous feeding in calm and turbulent environments, with emphasis on copepods. Marine Ecology Progress Series, 122 1995, pp. 135-145. https://doi.org/10.3354/meps122135
31. Brett M. T., and Müller-Navarra D. C., The role of highly unsaturated fatty acids in aquatic foodweb processes. Freshwater Biology, 38(3) 1997, pp. 483-499. https://doi.org/10.1046/j.1365-2427.1997.00220.x

Table A1 Food chain model description (based on Sato and Hayakawa [11]).

Phytoplankton Biomass:

$$\frac{dM_p}{dt} = G_p - P_p - E_p - R_p - D_p - O_p + IN_p \quad \text{(A1)}$$

$$G_p = g_p \cdot \left(1 - \frac{\gamma_{min,p}}{\gamma_p}\right) \cdot \exp(-\beta_p \cdot M_p) \cdot \frac{H_p}{H} \cdot M_p \quad \text{(A2)}$$

$$P_p = g_z \cdot \frac{M_p}{k_z + M_p} \cdot M_z \quad \text{(A3)}$$

$$E_p = e_p \cdot M_p \quad \text{(A4)}$$

$$R_p = (r_p + \varepsilon_p) \cdot M_p \quad \text{(A5)}$$

$$D_p = \frac{d_p}{H} M_p \quad \text{(A6)}$$

$$O_p = \frac{\sum_{j=1}^{n} V_{out,j}}{V} \cdot M_p \quad \text{(A7)}$$

$$IN_p = \frac{\sum_{j=1}^{n} V_{in,j} \cdot M_{p,j}}{V} \quad \text{(A8)}$$

Phytoplankton Nutrients:

$$\frac{dC_p}{dt} = \rho_p \cdot \frac{C_N}{k_p + C_N} \cdot \left(1 - \frac{\gamma_p}{k_{max,p}}\right) \cdot M_p - (P_p + E_p + R_p + D_p + O_p) \cdot \gamma_p + IN_p \cdot \gamma_{p,j} \quad \text{(A9)}$$

$$\gamma_p = \frac{C_p}{M_p} \quad \text{(A10)}$$

Zooplankton Biomass:

$$\frac{dM_z}{dt} = G_z - P_z - E_z - R_z - O_z + IN_z \quad \text{(A11)}$$

$$G_z = P_p \cdot \delta_z \quad \text{(A12)}$$

$$P_z = g_{f_1} \cdot \frac{M_z}{k_{f_1} + M_z} \cdot M_{f_1} \quad \text{(A13)}$$

$$E_z = \begin{cases} G_z \cdot (1 - \gamma_p/\gamma_z) & if \quad \gamma_z \geq \gamma_p \\ 0 & if \quad \gamma_z < \gamma_p \end{cases} \quad \text{(A14)}$$

$$R_z = (r_z + \varepsilon_z) \cdot M_z \quad \text{(A15)}$$

$$O_z = \frac{\sum_{j=1}^{n} V_{out,j}}{V} \cdot M_z \quad \text{(A16)}$$

$$IN_z = \frac{\sum_{j=1}^{n} V_{in,j} \cdot M_{z,j}}{V} \quad \text{(A17)}$$

Zooplankton Nutrients:

$$\frac{dC_z}{dt} = \begin{cases} G_z \cdot \gamma_p - (P_z + R_z + O_z - IN_z) \cdot \gamma_z & if \quad \gamma_z \geq \gamma_p \\ G_z \cdot \gamma_p - G_z(\gamma_p - \gamma_z) - (P_z + R_z + O_z) \cdot \gamma_z + IN_z \cdot \gamma_{z,j} & if \quad \gamma_z < \gamma_p \end{cases} \quad \text{(A18)}$$

$$\gamma_z = \frac{C_z}{M_z} \quad \text{(A19)}$$

Planktivorous Fish Biomass:

$$\frac{dM_{f_1}}{dt} = G_{f_1} - P_{f_1} - E_{f_1} - R_{f_1} \quad \text{(A20)}$$

$$G_{f_1} = P_z \cdot \delta_{f_1} \quad \text{(A21)}$$

$$P_{f_1} = g_{f_2} \cdot \frac{M_{f_1}}{k_{f_2} + M_{f_1}} \cdot M_{f_2} \quad \text{(A22)}$$

$$E_{f_1} = \begin{cases} G_{f_1} \cdot (1 - \gamma_z/\gamma_{f_1}) & if \quad \gamma_{f_1} \geq \gamma_z \\ 0 & if \quad \gamma_{f_1} < \gamma_z \end{cases} \quad \text{(A23)}$$

$$R_{f_1} = (r_{f_1} + \varepsilon_{f_1}) \cdot M_{f_1} \quad \text{(A24)}$$

Planktivorous Fish Nutrients:

$$\frac{dC_{f_1}}{dt} = \begin{cases} G_{f_1} \cdot \gamma_z - (P_{f_1} + R_{f_1}) \cdot \gamma_{f_1} & if \quad \gamma_{f_1} \geq \gamma_z \\ G_{f_1} \cdot \gamma_z - G_{f_1}(\gamma_z - \gamma_{f_1}) - (P_{f_1} + R_{f_1}) \cdot \gamma_{f_1} & if \quad \gamma_{f_1} < \gamma_z \end{cases} \quad \text{(A25)}$$

$$\gamma_{f_1} = \frac{C_{f_1}}{M_{f_1}} \quad \text{(A26)}$$

Piscivorous Fish Biomass:

$$\frac{dM_{f_2}}{dt} = G_{f_2} - E_{f_2} - R_{f_2} \quad \text{(A27)}$$

$$G_{f_2} = P_{f_1} \cdot \delta_{f_2} \quad \text{(A28)}$$

$$E_{f_2} = \begin{cases} G_{f_2} \cdot (1 - \gamma_{f_1}/\gamma_{f_2}) & if \quad \gamma_{f_2} \geq \gamma_{f_1} \\ 0 & if \quad \gamma_{f_2} < \gamma_{f_1} \end{cases} \quad \text{(A29)}$$

$$R_{f_2} = (r_{f_2} + \varepsilon_{f_2}) \cdot M_{f_2} \quad \text{(A30)}$$

Piscivorous Fish Nutrients:

$$\frac{dC_{f_2}}{dt} = \begin{cases} G_{f_2} \cdot \gamma_{f_1} - R_{f_2} \cdot \gamma_{f_2} & if \quad \gamma_{f_2} \geq \gamma_{f_1} \\ G_{f_2} \cdot \gamma_{f_1} - G_{f_2}(\gamma_{f_1} - \gamma_{f_2}) - R_{f_2} \cdot \gamma_{f_2} & if \quad \gamma_{f_2} < \gamma_{f_1} \end{cases} \quad \text{(A31)}$$

$$\gamma_{f_2} = \frac{C_{f_2}}{M_{f_2}} \quad \text{(A32)}$$

Nutrients:

$$\frac{dC_N}{dt} = L_N - O_N + DP_N + DZ_N + DF1_N + DF2_N - I_N \quad \text{(A33)}$$

$$L_N = \frac{L_{in}}{V} + \frac{\sum_{j=1}^{n} V_{in,j} \cdot C_{N,j}}{V} \quad \text{(A34)}$$

$$O_N = \frac{\sum_{j=1}^{n} V_{out,j}}{V} \cdot C_N \quad \text{(A35)}$$

$$DP_N = \{E_P + (P_p - G_z) + R_p\} \cdot \gamma_p \quad \text{(A36)}$$

$$DZ_N = \begin{cases} \{(P_z - G_{f_1}) + R_z\} \cdot \gamma_z & if \quad \gamma_z \geq \gamma_p \\ G_z \cdot (\gamma_p - \gamma_z) + \{(P_z - G_{f_1}) + R_z\} \cdot \gamma_z & if \quad \gamma_z < \gamma_p \end{cases} \quad \text{(A37)}$$

$$DF1_N = \begin{cases} \{(P_{f_1} - G_{f_2}) + R_{f_1}\} \cdot \gamma_{f_1} & if \quad \gamma_{f_1} \geq \gamma_z \\ G_{f_1} \cdot (\gamma_z - \gamma_{f_1}) + \{(P_{f_1} - G_{f_2}) + R_{f_1}\} \cdot \gamma_{f_1} & if \quad \gamma_{f_1} < \gamma_z \end{cases} \quad \text{(A38)}$$

$$DF2_N = \begin{cases} R_{f_2} \cdot \gamma_{f_2} & if \quad \gamma_{f_2} \geq \gamma_{f_1} \\ G_{f_2} \cdot (\gamma_{f_1} - \gamma_{f_2}) + R_{f_2} \cdot \gamma_{f_2} & if \quad \gamma_{f_2} < \gamma_{f_1} \end{cases} \quad \text{(A39)}$$

$$I_N = \rho_p \cdot \frac{C_N}{k_p + C_N} \cdot \left(1 - \frac{\gamma_p}{\gamma_{max,p}}\right) \cdot M_p \quad \text{(A40)}$$

Symbols:

$M_{i,j}$: biomass [gC m^{-3}], G_i : growth [gC m^{-3} day^{-1}], P_i : predation [gC m^{-3} day^{-1}], E_i:elimination [gC m^{-3} day^{-1}], R_i : respiration and mortality [gC m^{-3} day^{-1}], D_i : deposition [gC m^{-3} day^{-1}], O_i : outflow [gC m^{-3} day^{-1} OR gN m^{-3} day^{-1}], IN_i : biomass inflow [gC m^{-3} day^{-1}], V : water volume [m^3], H : water depth [m], H_i : compensation depth [m], $V_{out(in),j}$: water outflow [m^3 day^{-1}], g_i : maximum growth rate [day^{-1}], β_i : congestion effect constant [m^3 gC], k_i : half saturation constant [gC m^{-3} OR gN m^{-3}], e_i : exocytosis rate [day^{-1}], r_i : respiration rate [day^{-1}], ε_i : mortality rate [day^{-1}], d_i : deposition rate [m day^{-1}], δ_i : assimilation rate [-], C_i : nutrients concentration in water or biomass [gN m^{-3}], ρ_i : maximum nutrients uptake rate [gN gC^{-1} day^{-1}], L_{in} : inland nutrients inflow [gN day^{-1}], DN_i : biomass derived nutrients [gN day^{-1}], I_N : phytoplankton intake [gN m^{-3} day^{-1}], γ_i : N:C ratio [-], $\gamma_{max(min),i}$: maximum (minimum) N:C ratio [-], t : time [day], i : target subscripts (p : phytoplankton, z : zooplankton, f_1 : planktivorous fish, f_2 : piscivorous fish), n : number of adjacent sea area, j : sea area